Design, Structure−Activity Relationships, X-ray Crystal Structure, and Energetic Contributions of a Critical P1 Pharmacophore: 3-Chloroindole-7-yl-Based Factor Xa Inhibitors[⊥,‡]

Yan Shi,* Doree Sitkoff,* Jing Zhang, Herbert E. Klei, Kevin Kish, Eddie C.-K. Liu, Karen S. Hartl, Steve M. Seiler,[§] Ming Chang, Christine Huang, Sonia Youssef, Thomas E. Steinbacher, William A. Schumacher, Nyeemah Grazier, Andrew Pudzianowski, Atsu Apedo, Lorell Discenza, Joseph Yanchunas, Jr., Philip D. Stein, and Karnail S. Atwal[†]

Bristol-Myers Squibb Research & Development, P.O. Box 5400, Princeton, New Jersey 08543-5400

Received July 11, 2008

An indole-based P1 moiety was incorporated into a previously established factor Xa inhibitor series. The indole group was designed to hydrogen-bond with the carbonyl of Gly218, while its 3-methyl or 3-chloro substituent was intended to interact with Tyr228. These interactions were subsequently observed in the X-ray crystal structure of compound **18**. SAR studies led to the identification of compound **20** as the most potent FXa inhibitor in this series ($IC_{50} = 2.4$ nM, $EC_{2xPT} = 1.2$ μM). An in-depth energetic analysis suggests that the increased binding energy of 3-chloroindole-versus 3-methylindole-containing compounds in this series is due primarily to (a) the more hydrophobic nature of chloro- versus methyl-containing compounds and (b) an increased interaction of 3-chloroindole versus 3-methylindole with Gly218 backbone. The stronger hydrophobicity of chloro- versus methyl-substituted aromatics may partly explain the general preference for chloro- versus methyl-substituted P1 groups in FXa, which extends beyond the current series.

Introduction

Thromboembolic events are a leading cause of mortality worldwide.[1] However, only warfarin[2] is approved as an oral antithrombotic treatment in the U.S. Warfarin administration requires careful monitoring, as its plasma concentration levels can vary with patients' CYP2C9 genotype, diet, and coadministration of other drugs, leading to an increased risk of bleeding or thrombosis.[3] There is clearly an unmet need for oral anticoagulants with a better safety profile.

Factor Xa (FXa[a]), one of the serine proteases in the coagulation pathway, has been a target for antithrombotic development for some time.[4,5] FXa is involved in the initiation of coagulation when it is activated by the tissue factor/factor VIIa complex upon vascular injury. It also participates in the propagation stage of coagulation, catalyzing the cleavage of prothrombin to form the large burst of thrombin that is necessary for the final coagulation stage, clot formation.[6] Direct FXa inhibitors have been shown to be effective in animal models without causing a significant increase in bleeding,[7e,8b] and several compounds have progressed into late stage clinical trials.[7−10] Recent clinical trial disclosures on oral, direct FXa inhibitors such as razaxaban,[7] apixaban,[8] rivaroxaban,[9] and *N*-[(1*R*)-2-[4-(1-methyl-4-piperidinyl)-1-piperazinyl]-2-oxo-1-phenylethyl]-1*H*-indole-6-carboxamide (LY517717)[10] have provided clinical support for preclinical findings.

We have reported some of our efforts in developing orally active and selective FXa inhibitors.[11] The ketene aminal chemotype **2** (Scheme 1), which was derived from a high throughput screening (HTS) hit (compound **1**) by SAR development through parallel syntheses and optimization via medicinal chemistry, was attractive because of its nonpeptidic nature and charge neutrality. Many early FXa inhibitors containing charged benzamidine or guanidine moieties had poor oral bioavailability, and we hoped to avoid this problem with a neutral FXa inhibitor.[12] Compound **2** is a selective FXa inhibitor relative to related trypsin-like serine proteases and is active in rats after intravenous administration by measurement of ex vivo clotting time.[13]

While **2** and related FXa inhibitors containing a 2-methylbenzofuran group have many desirable properties, their potential for mutagenicity and/or CYP inhibition due to the benzofuran moiety limited our interest in these compounds.[14] In addition, the concentrations to double the prothrombin time (EC_{2xPT}) are on the order of 10^3 times higher than the corresponding IC_{50} values for this series.[11a] Several recent literature reports suggest that highly nonpolar coagulation factor inhibitors can have a tendency toward high protein binding.[15] This tendency could be associated with the relatively high concentrations required to achieve efficacy in plasma-based assays and presumably in vivo.[7a,12,16] The 2-methylbenzofuran moiety may contribute to the hydrophobic nature of compound **2** and result in its observed high EC_{2xPT} (19 μM). We thus sought to replace the 2-methylbenzofuran with a more hydrophilic pharmacophore while retaining the FXa inhibition activity, oral bioavailability, and other favorable properties of chemotype **2**.[11a]

Rational Design

On the basis of the X-ray crystal structure of a compound closely related to **2**, we used computer modeling to assist in identifying a replacement moiety. The starting point of design was the model of **2** in FXa (see Experimental Section).[11a] In this model (Figure 1), compound **2** adopts the commonly seen L-shaped conformation in the FXa active site. The acylpyrro-

[⊥] Dedicated to Professor William D. Wulff on the occasion of his 60th birthday.

[‡] The X-ray crystal structure coordinates of **18** in human factor Xa have been deposited in the Protein Data Bank (PDB code 3ens).

* To whom correspondence should be addressed. For Y.S.: phone, 609-818-4124; fax, 609-818-3456; e-mail, yan.shi@bms.com. For D.S.: phone, 609-818-5046; fax, 609-818-3545; e-mail, doree.sitkoff@bms.com.

[§] Deceased March 31, 2003.

[†] Deceased December 29, 2006.

[a] Abbreviations: FXa, factor Xa; CYP, cytochrome P450; PDB, Protein Data Bank; EC_{2xPT}, the concentration of inhibitor required to double the prothrombin based clotting time in human plasma; EDCI, 1-[3-(dimethylamino)propyl]-3-ethylcarbodiimide hydrochloride; tPA, tissue plasminogen activator.

10.1021/jm800855x CCC: $40.75
Published on Web 11/11/2008

Scheme 1

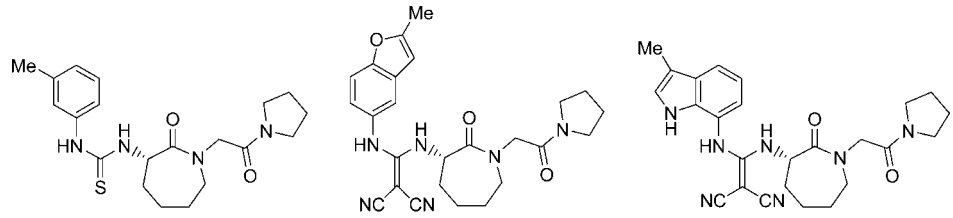

1 IC_{50} = 110 nM

2 IC_{50} = 30 nM, EC_{2xPT} = 19 μM

3

lidine fills the hydrophobic S4 pocket, and the caprolactam carbonyl oxygen forms a weak hydrogen bond with the backbone NH of Gly216 (N−O distance of 3.3 Å). One of the ligand's nitrile groups packs against the disulfide bond between Cys220 and Cys191 side chains. The 2-methylbenzofuran group fits in the S1 pocket of the active site, with the methyl group just above Tyr228. This interaction appears similar to that seen for chloroaryl P1 groups in several recently published crystal structures of serine proteases[17] and will be discussed later in further detail. The oxygen of the 2-methylbenzofuran does not have an explicit hydrogen bond partner, but its electron-withdrawing nature could enable the 3-CH to interact favorably with Asp189.[18]

We focused on satisfying two major interaction sites in the S1 pocket in our design. The first is the by now well-known hydrophobic interaction site above Tyr228, which is fully filled by the methyl group of the 2-methylbenzofuran in **2** and is often occupied by a nonpolar moiety in potent inhibitors of trypsin-like serine proteases that have a neutral P1 group.[5] The second interaction site, not satisfied in **2**, involves the carbonyl backbone of Gly218,[19] which could potentially accept a hydrogen bond from an appropriately placed donor in the ligand. Inhibitors containing basic P1 groups such as benzamidines commonly form a hydrogen bond to this carbonyl. At the time of our design, there were no known P1 pharmacophores that simultaneously achieved both the hydrophobic interaction with Tyr228 and a direct (non-water-mediated) hydrogen bonding interaction with Gly218 carbonyl.[20] We envisioned that a P1 pharmacophore with these properties could impart potency through the above interactions, while also improving pharmacological properties of the ligand relative to **2**, by increasing polarity (due to the hydrogen bond donor) and therefore potentially reducing protein binding.

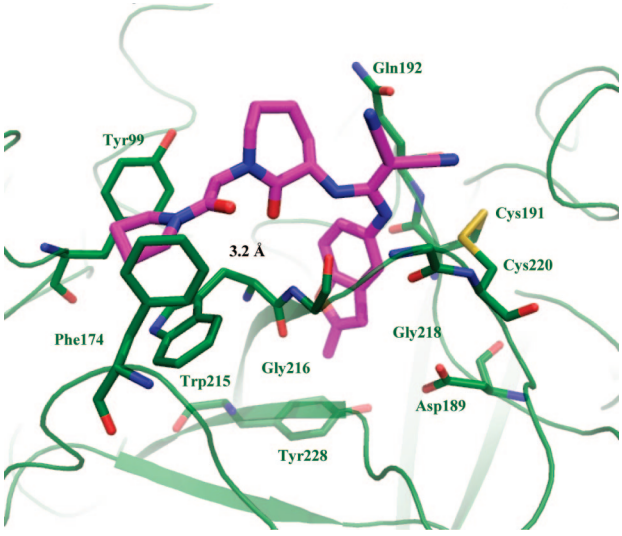

Figure 1. Binding model of **2** in FXa. Key residues are shown in stick representation, and the hydrogen bond between the ligand and Gly216 amide NH is highlighted. This and the following figures were created using PyMOL (http://www.pymol.org).

As a result of these considerations, we designed compound **3** (Scheme 1), which has a 3-methylindole in place of the 2-methylbenzofuran. The proposed binding model of **3** in FXa is shown in Figure 2. As can be seen in Figure 2a, the methyl group of the 3-methylindole overlays with the methyl group of 2-methylbenzofuran in **2** and should thus make similar interactions with Tyr228 in the S1 pocket of FXa, although it does not extend into the S1 pocket quite as far. Also, as intended by the design, the NH of the indole forms a slightly elongated hydrogen bond with the carbonyl group of Gly218 (3.3 Å, Figure 2b). In addition, compound **3** has a calculated log *P* of 2.42.[21] This value is 0.57 units lower than that of compound **2**, and therefore, **3** is predicted to be more hydrophilic than **2** (Table 1).

Chemistry

All the compounds reported in this work were prepared from their corresponding amines **6a**−**g** or their isothiocyanates **7a**−**g** and the caprolactam amine **8**.[11b] The amines **6a** and **6c**−**g** were obtained from their corresponding nitro compounds, which are either commercially available or readily prepared via known procedures.[22] The 3-methyl-7-aminoindole **6b** was synthesized by a two-step sequence from 7-nitro-1*H*-indole **4** as shown in Scheme 2. Formylation of indole **4** and one-step reduction of both the formyl and nitro groups with $NaBH_4$ afforded **6b** in 80% yield. The dicyano ketene aminals (**3**, **14**, and **15**) were prepared by sequential displacement of the two methylthio groups of 2-(bis(methylthio)methylene)malononitrile with 7-aminoindoles **6a**−**c** and the caprolactam amine **8** (Scheme 3). The ketene aminals **16**−**23** were prepared according to a one-pot procedure we developed for *N,N′*-disubstituted ketene aminals (Scheme 3).[23] For example, treatment of methyl 2-cyanoacetate (**10**) with sodium hydride and reaction of the resulting anion with 3-chloroindole-7-isothiocyanate **7c** afforded an intermediate thioamide anion (**12c**). Subsequent reaction of **12c** with caprolactam amine **8** and EDCI provided **18** (X = CO_2Me, Y = CH, Z = Cl) in 85% yield. The cyanoguanidine analogues **25** and **26** were prepared from a similar sequence according to a literature procedure (Scheme 4).[24] Treatment of the indole-7-isothiocyanates (**7b** and **7c**) with sodium cyanoamide gave the intermediates **24b** and **24c**, which were reacted with amine **8**

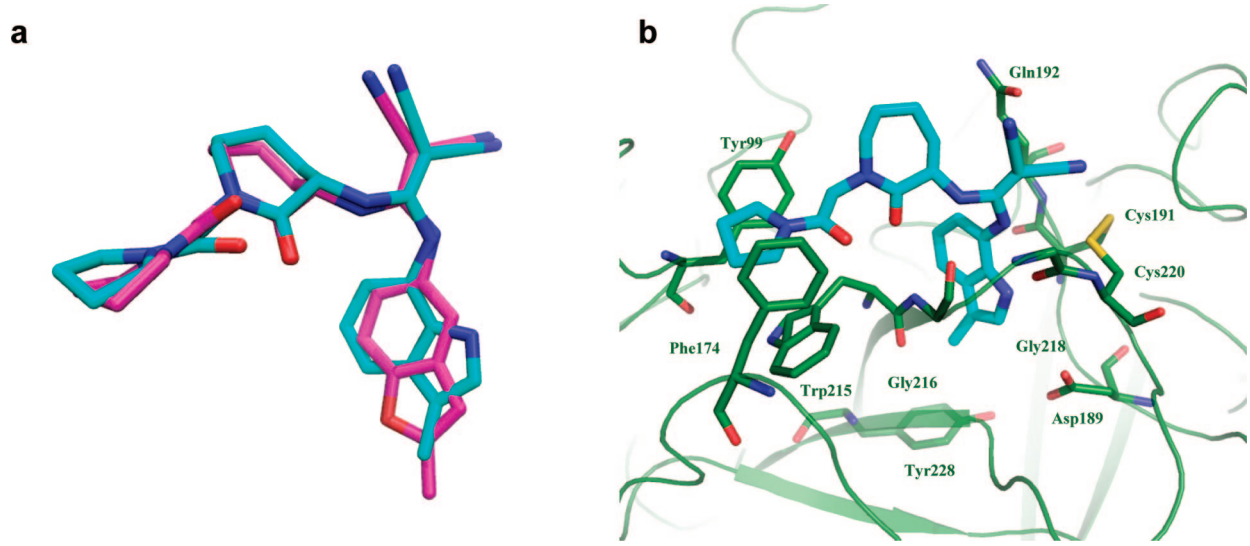

Figure 2. Model of the proposed compound **3** in FXa: (a) bound models of **2** (magenta carbons) and **3** (cyan carbons) superimposed in the FXa protein (not shown); (b) model of **3** in FXa. Key residues are shown in stick representation. The hydrogen bond between the ligand and Gly216 amide NH is highlighted, as is the designed hydrogen bond between the indole NH and Gly218 carbonyl.

and EDCI to afford **25** and **26**, respectively. The anti-FXa activity for compounds **2**, **3**, **14**−**23**, **25**, and **26** are shown in Table 1.

Results and Discussion

Although the proposed 3-methylindole compound **3** (IC_{50} = 114 nM) is about 4-fold less potent in FXa IC_{50} than **2**, it shows slight improvement in anticoagulation activity (EC_{2xPT} = 13 μM) compared to **2** (EC_{2xPT} = 19 μM). The des-methyl analogue **14** is about 4-fold less potent than **3**, which is similar to what was observed in the 2-methylbenzofuran series.[11a] The 3-chloro substituted indole compound **15** (IC_{50} = 9.3 nM) shows over 10-fold improvement in IC_{50} compared to **3** and is about 5-fold more potent in EC_{2xPT} (2.4 μM). The indole compound **3** (clogP = 2.42) was designed to be more polar than **2** (clogP = 2.99); this probably leads to a lower protein binding value for **3** (77%) in human plasma compared to **2** (92%). While the clogP of the 3-chloroindole compound **15** (clogP = 2.93) is very close to that of compound **2**, it has a slightly lower protein binding value (88%). The EC_{2xPT}/IC_{50} ratios for both compounds **3** (114) and **15** (258) are substantially lower than for **2** (633).

The effect of the different substituents at the 3 position of indole on anti-FXa activity was further examined with other ketene aminal linker series (compounds **16**−**23**) and in cyanoguanidine compounds **25** and **26**. The SAR are summarized as follows: (1) The 3-chloroindole compounds are always more potent than their 3-methylindole analogues (compare **15** to **3**, **20** to **19**, and **26** to **25**), with the 3-methylindole compounds having lower plasma protein binding values and EC_{2xPT}/IC_{50} ratios in each pair. (2) The indazole compound **17** (IC_{50} = 13700 nM) is about 30-fold less potent than the corresponding indole analogue **16** (IC_{50} = 650 nM), indicating the 2-nitrogen atom of indazole has an unfavorable interaction with FXa protein. (3) While the change of the 3-methylindole in compound **19** (IC_{50} = 118 nM) to 3-chloro- (**20**, IC_{50} = 2.4 nM) and 3-bromoindole (**21**, IC_{50} = 9 nM) improves FXa inhibition activity, the larger and more polar 3-cyano- (**22**, IC_{50} = 290 nM) and 3-carboxamide indole (**23**, IC_{50} = 17000 nM) analogues are far less potent. This is consistent with our modeling (vide supra) and X-ray crystal structure analysis of **18** (vide infra) in which the 3-chlorine atom is near Tyr228 and the size and polarity of the 3-substituent of the indole have a strong impact on anti-FXa activity. (4) The linker between the indole and caprolactam amine also has an important impact on anti-FXa activity. The ketene aminal compounds are more potent than their cyanoguanidine analogues. For example, all the 3-chloroindole ketene aminal compounds **15** (X = CN, IC_{50} = 9.3 nM), **18** (X = CO_2Me, IC_{50} = 8.9 nM), and **20** (X = $CONMe_2$, IC_{50} = 2.4 nM) are more potent than the 3-chloroindole cynanoguanidine **26** (IC_{50} = 46 nM). In addition, the activities of the chloroindole compounds are more sensitive to changes in the linker; replacing the ketene linker with a cyanoguanidine in the chloroindole case decreases potency by about 20-fold (compounds **20** and **26**), whereas in the methylindole case, potency is decreased by only about 3-fold (compounds **19** and **25**). Compound **20** is the most potent FXa inhibitor in this series, having IC_{50} = 2.4 nM and EC_{2xPT} = 1.2 μM.

X-ray Crystal Structure of 18 Bound to FXa. Figure 3 depicts the crystal structure of **18** in FXa, measured at 2.3 Å resolution. The ketene aminal adopts a typical syn−anti conformation[23] with the methyl ester anti to the 3-chloroindole group. The ketene and the aminal planes are significantly twisted (40°) along the elongated C=C bond (1.42 Å). As was intended by the design, the NH of the indole forms a hydrogen bond to the backbone carbonyl of Gly218 (2.8 Å). Also as expected from the modeling, the chlorine is slightly less deeply placed than the methyl group of 2-methylbenzofuran compound **2** and in other FXa compounds that contain a chlorine at the base of the S1 pocket (4.2 Å distance between chlorine and the Tyr228 C−OH atom for the crystal of **18** compared with a typical distance of 3.6 Å). This is consistent with the SAR observation that a hydrophobic and much larger 3-bromine atom (compound **21**, IC_{50} = 9 nM) can also be accommodated at this position, but the larger hydrophilic 3-cyano (compound **22**) and 3-carboxamide groups (compound **23**) are disfavored. The ester lies along the disulfide bond, with the carbonyl forming a hydrogen bond with the backbone NH of Gln192 (3.0 Å), in addition to its intramolecular interaction with the indole aminal NH (2.6 Å). The lactam carbonyl forms a hydrogen bond with Gly216 NH (3.0 Å) and with a crystallographic water molecule (3.1 Å); this water also participates in a hydrogen bond with the

Table 1. Human FXa Inhibitory Activity and Plasma Protein Bindings of **2**, **3**, **14**−**23**, **25**, and **26**

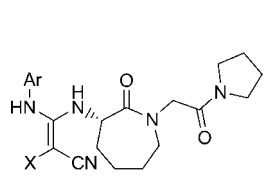

2, 3 and 14 - 23

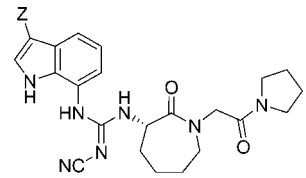

25: Z = Me
26: Z = Cl

compd	X	Ar	IC_{50} (nM)[a]	EC_{2xPT} (μM)[b]	EC_{2xPT}/IC_{50}	clogP[c]	protein binding (%)[d]
2	CN	2-methylbenzofuran-5-yl	30	19	633	2.99	92
3	CN	3-methyl-1*H*-indol-7-yl	114	13	114	2.42	77
14	CN	1*H*-indol-7-yl	430	>50			
15	CN	3-Cl-1*H*-indol-7-yl	9.3	2.4	258	2.93	88
16	COOMe	1*H*-indol-7-yl	650	50			
17	COOMe	1*H*-indazol-7-yl	13700	>50			
18	COOMe	3-Cl-1*H*-indol-7-yl	8.9	4.9	550		
19	$CONMe_2$	3-Me-1*H*-indol-7-yl	118	17	144	2.40	80
20	$CONMe_2$	3-Cl-1*H*-indol-7-yl	2.4	1.2	500	2.91	84
21	$CONMe_2$	3-Br-1*H*-indol-7-yl	9	6	667		
22	$CONMe_2$	3-cyano-1*H*-indol-7-yl	290	42	143		
23	$CONMe_2$	3-carboxamide-1*H*-indol-7-yl	17000	>50			
25		3-Me-1*H*-indol-7-yl	336	45	133	2.65	80
26		3-Cl-1*H*-indol-7-yl	46	15	326	3.09	84

[a] IC_{50} values are measured against human FXa utilizing the cleavage of a synthetic substrate S-2222. [b] Concentration of inhibitor required to double the prothrombin based clotting time in human plasma. [c] Biobyte clogP, version 4.2. [d] Protein binding in human serum by equilibrium dialysis ($n = 3$).

Scheme 2. Synthesis of Amine **6b** and Isothiocyanates **7a**−**g**[a]

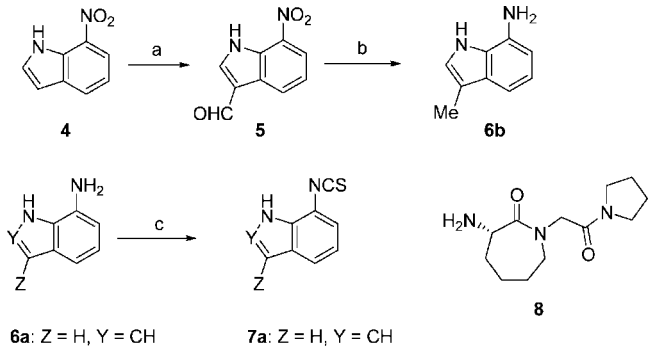

6a: Z = H, Y = CH
6b: Z = Me, Y = CH
6c: Z = Cl, Y = CH
6d: Z = H, Y = N
6e: Z = Br, Y = CH
6f: Z = CN, Y = CH
6g: Z = $CONH_2$, Y = CH

7a: Z = H, Y = CH
7b: Z = Me, Y = CH
7c: Z = Cl, Y = CH
7d: Z = H, Y = N
7e: Z = Br, Y = CH
7f: Z = CN, Y = CH
7g: Z = $CONH_2$, Y = CH

[a] Reagents and conditions: (a) DMF, $POCl_3$; (b) $NaBH_4$ (80% for two steps); (c) 1,1′-thiocarbonyldi-2(1*H*)-pyridone, CH_2Cl_2 (50−95%).

Scheme 3. Synthesis of **3** and **14**−**23**[a]

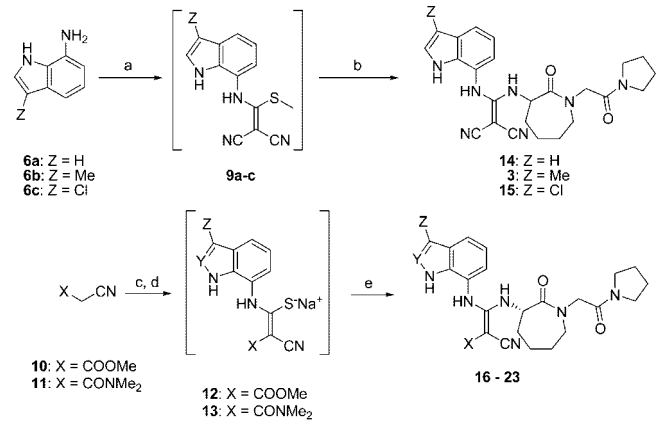

6a: Z = H
6b: Z = Me
6c: Z = Cl

9a-c

14: Z = H
3: Z = Me
15: Z = Cl

10: X = COOMe
11: X = $CONMe_2$

12: X = COOMe
13: X = $CONMe_2$

16 - 23

[a] Reagents and conditions: (a) 2-(bis(methylthio)methylene)malononitrile, EtOH, 70 °C; (b) **8**, EtOH, 70 °C (40−85% for two steps); (c) NaH, DMF; (d) **7a**−**g**, 60 °C; (e) **8**, EDCI (35−91%).

Scheme 4. Synthesis of **25** and **26**[a]

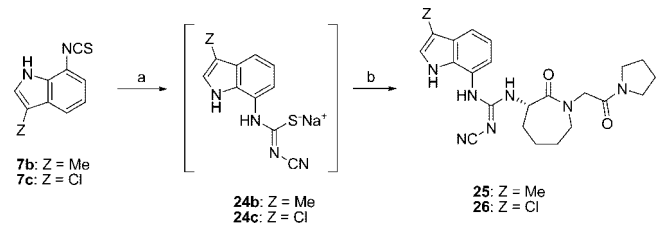

7b: Z = Me
7c: Z = Cl

24b: Z = Me
24c: Z = Cl

25: Z = Me
26: Z = Cl

[a] Reagents and conditions: (a) NaNHCN, DMF; (b) **8**, EDCI (83−87% for two steps).

side chain of Ser214. The pyrrolidine lies squarely in the S4 pocket. A surprising observation is that the Ser195 side chain oxygen is rotated toward His57 side chain rather than toward the ligand binding site, in a rare position/torsion angle.[25,26] This is presumably to accommodate the six-membered ring portion of the chloroindole, which is in proximity because of the linkage of the indole at its 7-position.

Chloro- versus Methyl-Substituted Indoles. In general, there is a dramatic increase in the anti-FXa activity of 3-chloro substituted indole compounds versus 3-methyl substituted indole compounds (compare **15** with **3**, **20** with **19**, **26** with **25**). This increased potency due to substitution of a methyl with a chlorine varies from 7- to 50-fold, corresponding to a difference in binding energy of 1−2.3 kcal/mol at room temperature. A preference for chlorine over methyl at the position above Tyr228 has been noted in other chemotypes as well.[16c,18b,27] Significantly, there are vastly more examples of FXa inhibitors in the literature that contain chlorine atoms at this position in the P1 pocket versus a methyl group, although the two groups are commonly considered to be of fairly similar size and hydrophobicity. The source of the binding energy associated with the chlorine atom has been ascribed to (a) lipophilic interactions,[17b,28] (b) a positive electrostatic potential at the tip of the chlorine atom which interacts favorably with the π-electrons of Tyr 228,[18b,20] (c) polarization of the C−H bond ortho to the chloro

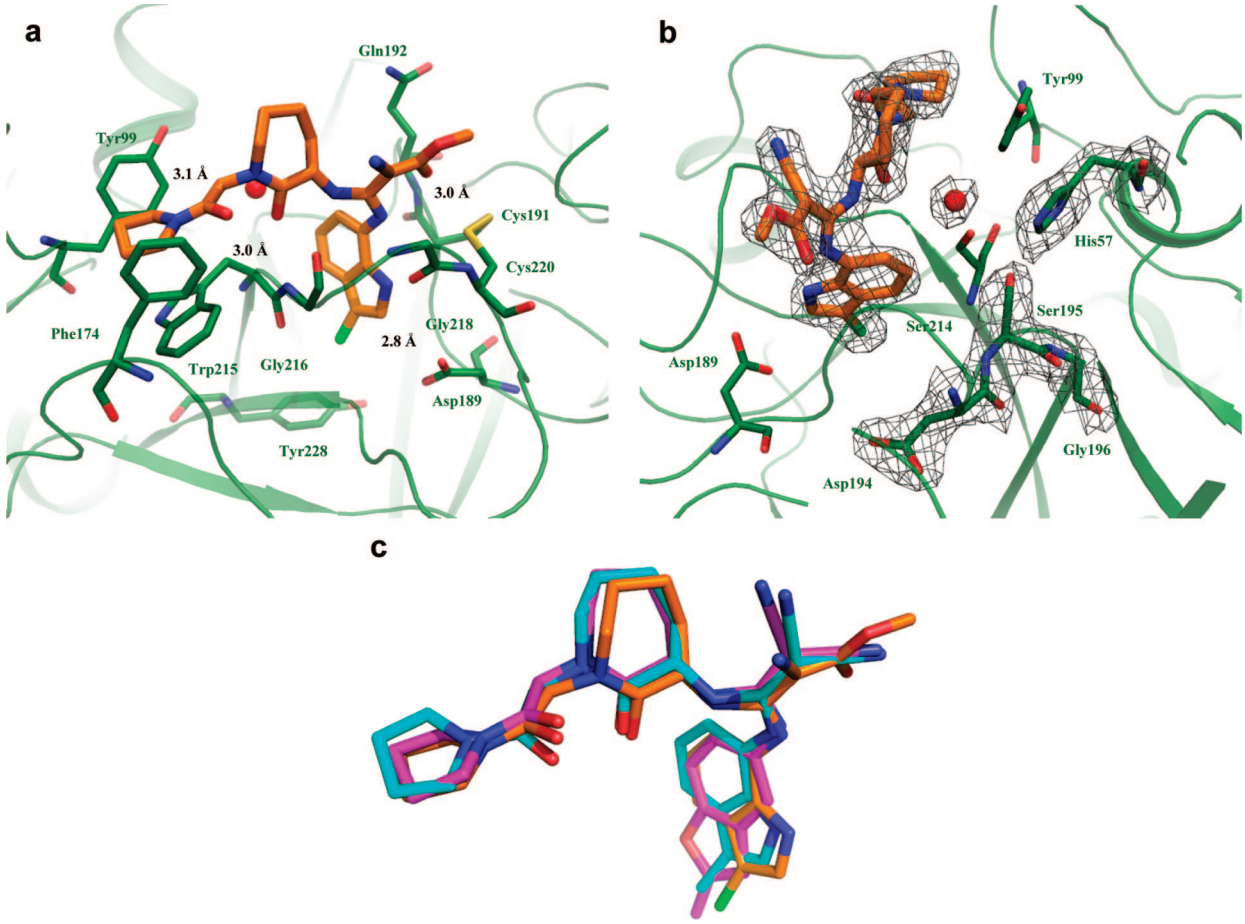

Figure 3. (a) Crystal structure of **18** bound in FXa. Hydrogen bonds between the ligand and protein partners Gly218 backbone carbonyl, Gln192 backbone amide NH, and Gly216 backbone amide NH are highlighted, as is a hydrogen bond between the ligand's lactam carbonyl and a crystallographic water molecule (red sphere). (b) Alternative view of bound X-ray crystal structure of **18**. The $2F_o - F_c$ electron density contoured at 1σ is shown for Ser195 and surrounding residues, supporting the unusual torsion of Ser195 side chain oxygen toward His57 rather than toward the ligand. The hydrogen bond interactions between the crystallographic water and the ligand/protein are also shown. (c) X-ray crystal structure of **18** (orange carbons) overlaid with the bound models of **2** (magenta carbons) and **3** (cyan carbons) (protein not shown).

substituent, leading to a favorable interaction with the nearby Asp189,[18] and (d) favorable dispersion interactions with the π-electrons of Tyr228.[29a] As yet, however, few studies have critically and quantitatively examined or rank-ordered the reasons for the apparent preference for chlorine over methyl in the FXa S1 pocket. In the following sections, we present quantitative calculations and examine relevant experimental data with the goal of rationalizing the difference between the activities of the methyl- and chloro-substituted indole compounds in the current series.

Quantum Chemical Calculations. To probe which residues in FXa are responsible for the difference in binding energy of the chloro versus methyl compounds, quantum chemical interaction energies were calculated between an isolated chloroindole or methylindole ligand fragment and various nearby residue fragments from FXa. The residue fragments selected for analysis were the Tyr228 side chain (modeled by *p*-cresol), the Asp189 side chain (modeled by acetic acid), and the backbone carbonyl of Gly218 (modeled by *N*-methylacetamide). The calculations involving the Asp189 side chain were performed for both the ionized and neutral forms of the side chain. According to the crystal structure of **18**, the carboxylate is in very close contact with the ligand but does not have a salt bridge or ion partner, so the neutral form could be energetically favored when the ligand is bound due to desolvation penalties for burying charged species. The results of these calculations, shown in Table 2,

Table 2. MP2 Quantum Chemical Interaction Energies (kcal/mol) between Isolated FXa Residue Surrogates and the 3-Chloroindole or 3-Methylindole Fragment of **18** in Its Bound Conformation

FXa residue surrogate	$\Delta H_{\text{chloroindole}}$ [a]	$\Delta H_{\text{methylindole}}$ [b]	$\Delta\Delta H$ [c]
Tyr228 side chain	−0.67	−0.63	−0.04
Asp189 side chain (charged)	−11.62	−12.11	0.49
Asp189 side chain (neutral)	−1.03	−0.31	−0.72
Gly218 carbonyl	−5.43	−4.39	−1.04

[a] Calculated heat of formation of the 3-chloroindole−residue complex minus heats of formation of the 3-chloroindole and FXa residue alone. [b] Calculated heat of formation of the 3-methylindole−residue complex minus heats of formation of the 3-methylindole and FXa residue alone. [c] $\Delta\Delta H = \Delta H_{\text{chloroindole}} - \Delta H_{\text{methylindole}}$.

demonstrate that all of the FXa residue fragments interact favorably with both the 3-chloro- and 3-methylindole (see $\Delta H_{\text{chloroindole}}$ and $\Delta H_{\text{methylindole}}$ interaction energy columns). The residue fragment with the largest interaction energies is the charged Asp189 side chain, followed by the Gly218 carbonyl; the Tyr228 and Asp189 neutral side chains have the smallest interaction energies. As noted in the relative interaction energies column ($\Delta\Delta H$) of Table 2, the Tyr228 side chain shows virtually no preference for 3-chloroindole versus 3-methylindole. Instead, the FXa residue fragment most responsible for the preferred binding of 3-chloroindole over 3-methylindole is the Gly218 backbone carbonyl; presumably the hydrogen bond between the Gly218 backbone carbonyl and the indole NH, or the electrostatic interaction in general is strengthened when the electron-

withdrawing chlorine is substituted for the electron-donating methyl group on the indole ring. This is consistent with the observation that changing the ketene linker to a cyanoguanidine linker has a more dramatic effect on FXa potency in chloroindole (**20** and **26**) versus methylindole (**19** and **25**) compounds (vide supra); differences in linker geometry could influence the indole N<u>H</u>−Gly218C=<u>O</u> interaction. The Asp189 charged side chain actually shows a preference for 3-methylindole over 3-chloroindole, in contrast to the expectation based on Cl- versus Me-induced polarization of the indole 2C−H bond. However, the neutral version of the Asp189 side chain favors 3-chloroindole over 3-methylindole, in agreement with the experimental findings. In summary, the quantum calculations suggest that the preference for 3-chloroindole over 3-methylindole is due to enhanced interactions between the ligand and the backbone carbonyl of Gly218 but not due to changes in interactions with Tyr228. In addition, calculations indicate the chloroindole to interact more favorably with the neutral form of Asp189 side chain than does the methylindole, raising the possibility of a significant pK_a shift of Asp189 when these ligands are bound.

It should be noted that the chlorine or methyl group on the 7-linked 3-substituted indole ligand studied here is considerably farther from Tyr228 than are the chlorines in most chloro-P1 groups (4.2 Å versus 3.6 Å), which could explain the insensitivity of the calculated Tyr228-ligand interaction energy to the chloro versus methyl substitution. Interestingly, in a recent study of Cl−π interactions in simplified systems,[29a] dispersion was highlighted as the major contributor for the Cl-ethyne/benzene interaction at ∼3.5 Å, i.e., near the minimum of the interaction energy curve. The calculated interactions decrease with distance for both the Cl-ethyne/benzene and the methane/benzene pairs;[29a−c] however, more detailed comparisons to that work are difficult, as the model systems differ from those studied here. Notably, a previous, similar assessment of a more typically positioned chlorine-containing P1 ligand in FXa found that interactions with Tyr228 actually slightly disfavored binding of the chlorine- versus methyl-containing ligands; in that case, interactions with the charged Asp189 residue favored the chloro- versus methyl-P1 group.[18a]

As mentioned above, the preference for chlorine over methyl substituents in the S1 pocket has previously been attributed to a positive electrostatic potential at the tip of the chlorine in chlorobenzene which might interact favorably with the π-electrons of Tyr228. Rather than estimating interactions based on ligand surface potentials, the quantum method used here computes total interaction energies between the two molecular fragments. Additionally, the quantum energies are calculated at a higher level of theory, permitting a more reliable quantitative estimate of the interaction between Tyr228 and the chloro versus the methyl substituent.

Desolvation Contributions. The experimental measurements of protein binding (Table 1) are higher for the 3-chloroindole compounds versus their 3-methylindole counterparts, indicating that the chloroindole-containing compounds are likely more hydrophobic (compare **15**, **20**, and **26** with **3**, **19**, and **25**). Higher hydrophobicity indicates that desolvation contributions favor removal from water and therefore binding of the chlorine-containing ligands, in agreement with the observed increased binding of chlorine- versus methyl-containing compounds to FXa. Additionally, the ratios of EC_{2xPT} to IC_{50} increase upon replacement of a methyl with a chloro group (Table 1), again suggesting that the chlorine-containing ligands are more hydrophobic and are likely easier to desolvate. Experimental and calculated log *P* values are shown for compounds **3**, **15**, **19**, **20**, **25**, **26**, and several relevant small molecules in Tables 1 and 3. The log *P* and clogP differences between each matched pair of chlorine versus methyl-containing compounds in this group range from 0.15 to 0.51, corresponding to a 0.2−0.7 kcal/mol desolvation contribution that consistently favors binding of the chlorine-containing compounds. This amount is less than the observed 1−2.3 kcal/mol preference based on measured FXa IC_{50} values in the current series; thus, desolvation by itself only partially explains why chloro compounds are favored in FXa over their methyl-containing counterparts for this series. However, we note that a stronger hydrophobicity, and thus a more favorable desolvation contribution, is likely at least part of the reason that chloro-, rather than methyl-, substituted aromatics are commonly preferred in the S1 pocket in general.

Table 3. The log *P* and clogP Values for Compounds Containing an Arylmethyl versus an Arylchlorine Group

compd	exptl log P_{oct}[a]	clogP[b]
toluene	2.69	2.64
chlorobenzene	2.84	2.86
3-methylindole	2.60	2.63
3-chloroindole		3.07

[a] Hansch, C.; Leo, A. *Substituent Constants for Correlation Analysis in Chemistry and Biology*; Wiley: New York, 1979. [b] Biobyte clogP, version 4.2.

Table 4. Selectivity Profiles of **15** and **20**

	IC_{50} (nM) or % inhibition at 33 μM	
human enzymes	**15**	**20**
factor Xa	9.3	2.4
trypsin	10813	1043
thrombin	7360	1100
tryptase	27%	13%
activated protein C	>33000	>33000
factor IXa	32%	17%
factor VIIa	>33000	>33000
urokinase	>33000	>33000
plasmin	11%	32%
tPA	3990	45%

In Vivo Activity. The ketene aminals described above are selective FXa inhibitors relative to related trypsin-like serine proteases. Table 4 shows the activity profiles of compounds **15** and **20**. Furthermore, compound **15** partially protected against lethality in mice induced by intravenous injection of Russel's viper venom (which causes FXa activation and lethality due to pulmonary thrombosis). Vehicle-treated mice died within 2.4 ± 0.3 min (n = 22) after the Russel's viper venom injection, while survival times were increased to 18.0 ± 5.2 min (n = 4) after oral administration of 5 mg/kg **15**.[30]

Conclusion

We have reported here the design and incorporation of an indole-based P1 moiety onto a previously established FXa inhibitor series. The indole group was designed and subsequently observed in an X-ray crystal structure to achieve a hydrogen bond with the backbone carbonyl of Gly218. While there have been previous reports of indoles as P1 groups,[20,31] this is the first report of a series of FXa inhibitors linked at the 7-position of indole, which causes the primary hydrogen bond partner to be Gly218 in place of Asp189, and the Ser195 side chain to move into a rarely seen torsional position. The new torsion angle creates a slightly larger and more hydrophobic pocket which could be capitalized upon in future ligand designs. An in-depth energetic analysis suggests that the increased binding energy of 3-chloroindole versus 3-methylindole-containing compounds in this series is due primarily to (a) the more hydrophobic nature

of chloro- versus methyl-containing compounds, which makes them easier to desolvate, and (b) increased interactions of 3-chloro- versus 3-methyl-containing indoles with Gly218 backbone. Interactions with Asp189 may play a secondary role. The Tyr228 interacts well with both 3-chloroindoles and 3-methylindoles without special preference. The stronger hydrophobic nature of chloro- versus methyl-substituted aromatic rings may explain in part the general preference for chloro- versus methyl-substituted P1 groups in FXa, which extends beyond the current series. These calculations have led to a deeper understanding of the role played by chlorine in indole- as well as nonindole-containing ligand−FXa interactions.

Experimental Section

Generation of Binding Models. Models were obtained by minimizing ligands **2** and **3** in the published FXa crystal structure 1fjs[32] using a distance-dependent dielectric in Discover, version 98.0, in the InsightII package (Accelrys, Inc., San Diego, CA) with the CFF force field.[33] The ligand was initially placed in the FXa active site based on an in-house crystal structure of a compound identical to **2** but with an acylguanidine linker in place of the ketene aminal.[11a] The ligand and all residues in the protein were held fixed with the exception of Tyr99, Phe174, Cys191, Cys220, Trp215, Ser195, Gln192, Arg143, Glu146, and Gly218. Following convergence, the minimization was repeated with the ligand free to move.

Calculation of Quantum Mechanical Interaction Energies. All molecules were minimized separately in the gas phase in the Jaguar program[34] (Schrödinger, LLC) using ab initio density functional theory B3LYP/6-31G*. Subsequently, either chloroindole or methylindole was placed near the molecule representing the side chain or backbone moiety of interest in a geometry taken from the crystal structure of **18** (for 3-methylindole, the indole was fixed to its position in the crystal structure of **18**). The interaction energies were calculated with fixed geometries at the MP2 level with basis set 6-311+G** using Gaussian[35] with counterpoise (CP) corrections.

Crystallization of FXa with Compound 18. When complexed with the inhibitor, the protein stock solution consisted of FXa at 9.8 mg/mL (0.27 mM based on the calculated molecular weight of 36.1 kDa) in 20 mM Tris-HCl at pH 7.5, 150 mM NaCl, 5% v/v DMSO, and 100 μM compound **18**. All co-crystallization trials of FXa were prepared by the hanging-drop, vapor-diffusion method. The initial crystallization screens, which were prepared on a Cyberlab/Gilson C-240 (Middleton, WI) in NeuroProbe (Gaithersburg, MD) CT300L2/5 trays, consisted of several commercial kits from Hampton Research (Aliso Viejo, CA).

The initial crystals were observed from solution 26 of Crystal Screen 2 and were further optimized on siliconized cover slips in 24-well Linbro plates. The 1 mL reservoir solution consisted of 15−22% w/v PEG MME 5000, 10 mM calcium acetate, 350 mM sodium acetate, 100 mM lithium sulfate, and 100 mM MES pH 6.0. Drops were formed from 1 μL of the protein solution and 1 μL of the reservoir solution (total initial drop volume of 2 μL), mixed, and equilibrated at room temperature. Crystals appeared within 1 week. Single crystals were removed and prepared for data collection with 20% v/v glycerol added to the reservoir solution as the cryoprotectant. The diffraction pattern from crystals gave unit cell parameters of $a = 62.3$ Å, $b = 78.9$ Å, $c = 73.9$ Å, and $\beta = 102.8°$. The symmetry was consistent with space group $P2_1$. On the basis of the unit cell and space group, the asymmetric unit was estimated to contain two FXa molecules (50% solvent fraction).

Structure Refinement. Diffraction images were recorded on a R-axis IV++ image plate detector mounted on a Rigaku RU-200 X-ray generator run at 50 kV and 100 mA (5 kW) with Osmic "blue" confocal optics. A collimator with 0.3 mm × 0.6 mm pinholes was used to collimate the Cu Kα beam. An Oxford Cryosystems model 600 liquid-nitrogen cooler maintained the mounted crystal at 100 K. The diffraction images were processed with DENZO and SCALEPACK from the HKL[36] suite. The intensities were converted to structure-factor amplitudes and placed on an absolute scale with TRUNCATE[37] from the CCP4[38] suite. An earlier in-house structure, with its inhibitor and waters removed, was used as the initial model. The structure was first refined to 2.3 Å resolution with CNX[39] (Accelrys, Inc., San Diego, CA) and modeled with QUANTA (Accelrys, Inc., San Diego, CA). The refinement was completed with PHENIX,[40] modeled with COOT,[41] and checked with MolProbity.[42] Ligand parametrization was done with eLBOW;[40] however, the target length of the vinyl bond was set to 1.41 Å based on the structures of similar compounds[23] and QChem 3.0[43] RI-MP2/6-31+G(d,p) ab initio calculations on the truncated structure (*Z*)-methyl 2-cyano-3-(methylamino)-3-(phenylamino)acrylate. The measured structure factors and refined coordinates were deposited in the Protein Data Bank[44] as PDB entry 3ens.

Chemistry. All reagents and solvents were of commercial quality and used without further purification. Column chromatography was performed using Merck silica gel 60 (230−400 mesh). Proton NMR spectra (500 MHz) and carbon NMR (126 MHz) were obtained on a Joel 500 spectrometer. Chemical shifts are reported in parts per million relative to $CDCl_3$ (7.26 ppm for proton and 77.00 ppm for carbon NMR). All new final SAR compounds were determined to be consistent with the proposed structures by ^{1}H and ^{13}C NMR, MS, HRMS, and combustion elemental analysis.

General Procedure for the Synthesis of Compounds 2, 3, 14, and 15. A solution of 2-(bis(methylthio)methylene)malononitrile (42.5 mg, 0.25 mmol) and 1*H*-indol-7-amine **6a** (36.3 mg, 0.28 mmol) in absolute ethanol (1.5 mL) was stirred at 70 °C for 6 h. The caprolactam amine **8** (60 mg, 0.25 mmol) was added, and the reaction mixture was stirred at 70 °C overnight. The mixture was then concentrated to dryness and the residue was purified by flash chromatography on silica gel (0−5% methanol in ethyl acetate) to afford compound **14** as a yellow solid (44.5 mg, 40% yield).

General Procedure for the Synthesis of Compounds 16−23, 25, and 26. To a solution of methyl 2-cyanoacetate (24.8 mg, 0.25 mmol) in dry DMF (1.5 mL) was added NaH (95%, 8.2 mg, 0.33 mmol). The mixture was stirred for 10 min at room temperature, upon which time 3-chloro-7-isothiocyanato-1*H*-indole **7c** (47 mg, 0.23 mmol) was added in one portion. The mixture was stirred for 30 min at 60 °C, and the HPLC analysis showed the disappearance of 3-chloro-7-isothiocyanato-1*H*-indole. The caprolactam amine **8** (60 mg, 0.25 mmol) and 1-(3-dimethylaminopropyl)-2-ethylcarbodiimide hydrochloride (58 mg, 0.30 mmol) were added in that order. The reaction mixture was stirred at room temperature overnight. The reaction was then quenched by addition of 10% of lithium chloride solution (2 mL) and extracted with ethyl acetate three times (3 × 10 mL). The combined organic fractions were washed once with brine, dried over $MgSO_4$, and evaporated. The residue was purified by flash chromatography on silica gel (0−5% methanol in ethyl acetate) to afford compound **18** as a yellow solid (116 mg, 91% yield). The products were analyzed with HPLC with following method: column-YMC S-5 ODS-A, 4.6 mm × 50 mm; detection at 220 nm; flow rate 4 mL/min; 4 min linear gradient from 10:90 methanol/water (containing 0.2% phosphoric acid) to 90:10 methanol/water (containing 0.2% phosphoric acid).

(*S*)-2-((2-Methylbenzofuran-5-ylamino)(2-oxo-1-(2-oxo-2-(pyrrolidin-1-yl)ethyl)azepan-3-ylamino)methylene)malononitrile (2). This compound was prepared in 95% yield from 2-methylbenzofuran-5-amine, 2-(bis(methylthio)methylene)malononitrile, and **8**. ^{1}H NMR ($CDCl_3$) δ 7.40 (d, 1H, $J = 8.2$ Hz), 7.25 (s, 1H), 7.09 (s, 1H), 6.96 (d, 2H, $J = 6.6$ Hz), 6.36 (s, 1H), 4.90 (br s, 1H), 4.06 (s, 2H), 3.60 (t, 1H, $J = 11.8$ Hz), 3.40 (t, 2H, $J = 6.9$ Hz), 3.30 (t, 2H, $J = 6.9$ Hz), 3.16 (dd, 1H, $J = 13.2$, 3.3 Hz), 2.43 (s, 3 H), 2.15 (d, 1H, $J = 13.2$ Hz), 2.06 (br s, 1H), 1.55−1.95 (m, 8H) ppm; ^{13}C NMR (126 MHz, $CDCl_3$) δ 171.86, 165.47, 160.01, 157.66, 153.78, 130.73 (2C), 128.62, 121.37, 118.21, 117.93, 112.03, 102.88 (2C), 53.99, 51.64, 50.57, 46.04, 45.60, 31.02, 26.33, 26.10, 25.62, 23.98, 14.11 ppm. HRMS for $C_{25}H_{28}N_6O_3$ calcd for $(M + H)^+$, 461.2301; measured, 461.2303. Anal. ($C_{25}H_{28}N_6O_3$) C, H, N.

(*S*)-2-((3-Methyl-1*H*-indol-7-ylamino)(2-oxo-1-(2-oxo-2-(pyrrolidin-1-yl)ethyl)azepan-3-ylamino)methylene)malononitrile (3). This compound was prepared in 85% yield from **6b**, **8**, and 2-(bis(methylthio)methylene)malononitrile. ^{1}H NMR ($CDCl_3$) δ 9.38 (s, 1H), 7.47 (d, 1H, J = 8.2 Hz), 7.30 (s, 1H), 7.01 (t, 1H, J = 7.7 Hz), 6.92 (s, 1H), 6.81 (d, 1H, J = 7.7 Hz), 6.32 (d, 1H, J = 5.0 Hz), 4.72 (br s, 1H), 4.0−4.12 (m, 2H), 3.69 (s, 3H), 3.47 (br s, 1H), 3.33−3.40 (m, 2H), 3.30 (t, 2H, J = 6.6 Hz), 3.12 (d, 1H, J = 6.0 Hz), 2.26 (s, 3 H), 1.40 −1.92 (m, 10H) ppm; ^{13}C NMR (126 MHz, $CDCl_3$) δ 172.12, 165.81, 164.92, 131.25, 130.91, 123.23, 119.36, 119.26, 119.06, 116.86, 116.65, 116.03, 112.35, 54.74, 52.01, 50.37, 46.12, 45.72, 30.49, 26.22, 26.10, 26.00, 24.00, 9.66 ppm. HRMS for $C_{25}H_{29}N_7O_2$ calcd for $(M + H)^+$, 460.2461; measured, 460.2463. Anal. ($C_{25}H_{29}N_7O_2$) C, H, N.

(*S*)-2-((1*H*-Indol-7-ylamino)(2-oxo-1-(2-oxo-2-(pyrrolidin-1-yl)ethyl)azepan-3-ylamino)methylene)malononitrile (14). This compound was prepared in 40% yield from **6a**, **8**, and malononitrile. ^{1}H NMR (500 MHz, $CDCl_3$) δ 9.93 (s, 1 H), 7.59 (d, J = 7.9 Hz, 1 H), 7.48 (s, 1 H), 7.21 (s, 1 H), 7.07 (t, J = 7.5 Hz, 1H), 6.92 (d, J = 7.5 Hz, 1 H), 6.54 (s, 1 H), 6.35 (s, 1H), 5.25 (s, 1H), 4.75 (s, 1H), 4.12 (s, 1 H), 3.19−3.60 (m, 6 H),1.39−1.90 (m, 10 H) ppm. HRMS for $C_{24}H_{27}N_7O_2$ calcd for $(M + H)^+$, 446.2305; measured, 446.2304. Anal. ($C_{24}H_{27}N_7O_2$) C, H, N.

(*S*)-2-((3-Chloro-1*H*-indol-7-ylamino)(2-oxo-1-(2-oxo-2-(pyrrolidin-1-yl)ethyl)azepan-3-ylamino)methylene)malononitrile (15). This compound was prepared in 79% yield from **6c**, **8**, and 2-(bis(methylthio)methylene)malononitrile. ^{1}H NMR (500 MHz, $CDCl_3$) δ 10.10 (s, 1H), 7.61 (s, 1H), 7.52 (d, 1H, J = 8.3 Hz), 7.04−7.12 (m, 2H), 6.92 (d, 1H, J = 7.2 Hz), 6.34 (s, 1H), 4.73 (s, 1H), 4.15 (d, 1H, J = 16.5 Hz), 3.96 (d, 1H, J = 14.9 Hz), 3.49 (m, 1H), 3.26−3.34 (m, 1H), 3.19−3.27 (m, 2H), 3.05−3.19 (m, 2H, J = 16.8 Hz), 1.39−1.90 (m, 10H) ppm; ^{13}C NMR (126 MHz, $CDCl_3$) δ 172.34, 165.81, 165.59, 129.94, 129.58, 127.69, 122.66, 120.90, 120.56, 119.95, 118.37, 117.87, 117.64, 106.60, 55.02, 52.15, 50.49, 46.12, 45.74, 30.53, 26.26, 26.16, 26.02, 23.94 ppm. HRMS for $C_{24}H_{26}ClN_7O_2$ calcd for $(M + H)^+$, 480.1915; measured, 480.1910. Anal. ($C_{24}H_{26}ClN_7O_2$) C, H, Cl, N.

(*S*)-Methyl-3-(1*H*-indol-7-ylamino)-2-cyano-3-(2-oxo-1-(2-oxo-2-(pyrrolidin-1-yl)ethyl)azepan-3-ylamino)acrylate (16). This compound was prepared in 67% yield from **7a**, **8**, and methyl 2-cyanoacetate. ^{1}H NMR ($CDCl_3$) δ 11.03 (s, 1H), 9.64 (s, 1H), 7.60 (d, 1H, J = 8.3 Hz), 7.13 (t, 1H, J = 7.4 Hz), 7.02 (d, 1H, J = 7.7 Hz), 6.56 (s, 1H), 6.17 (br s, 1H), 5.21 (br s, 1H), 4.14−4.34 (m, 1H), 3.96 (d, 1H, J = 15 Hz), 3.77 (s, 3H), 3.30−3.47 (m, 6H), 3.12−3.18 (m, 1H), 1.21−1.96 (m, 10H) ppm; ^{13}C NMR ($CDCl_3$) δ 173.82, 170.22, 165.85, 164.17, 131.07, 130.20, 125.59, 120.66, 120.25, 120.08, 119.42, 117.20, 116.90, 103.23, 54.90, 52.01, 51.52, 50.19, 46.06, 45.74, 42.78, 40.99, 30.71, 26.16, 24.04 ppm. HRMS for $C_{25}H_{30}N_6O_4$ calcd for $(M + H)^+$, 479.2407; measured, 479.2401. Anal. ($C_{25}H_{30}N_6O_4$) C, H, N.

(*S*)-Methyl-3-(1*H*-indazol-7-ylamino)-2-cyano-3-(2-oxo-1-(2-oxo-2-(pyrrolidin-1-yl)ethyl)azepan-3-ylamino)acrylate (17). This compound was prepared in 50% yield from **7d**, **8**, and methyl 2-cyanoacetate. ^{1}H NMR ($CDCl_3$) δ 11.07 (s, 1H), 9.76 (s, 0.5H), 8.06 (s, 1H), 7.47−7.68 (m, 1H), 7.00−7.16 (m, 2H), 6.03 (br s, 0.5H), 5.05 (s 1H), 4.02−4.05 (m, 1H), 3.78 (s, 3H), 6.60−3.68 (m, 1H), 3.22−3.45 (m, 6H), 3.03−3.17 (m, 1H), 1.21−1.95 (m, 10H) ppm; ^{13}C NMR ($CDCl_3$) δ 172.73, 170.95, 159.26, 155.60, 137.76, 133.36, 123.95, 121.61, 120.72, 119.61, 116.37, 110.43, 104.60, 54.96, 51.64, 50.63, 50.05, 46.16, 45.80, 30.63, 30.35, 29.70, 26.12, 24.02 ppm. HRMS for $C_{24}H_{29}N_7O_4$ calcd for $(M + H)^+$, 480.2359; measured, 480.2359. Anal. ($C_{24}H_{29}N_7O_4$) C, H, N.

(*S*)-Methyl-3-(3-chloro-1*H*-indol-7-ylamino)-2-cyano-3-(2-oxo-1-(2-oxo-2-(pyrrolidin-1-yl)ethyl)azepan-3-ylamino)acrylate (18). This compound was prepared in 91% yield from **7c**, **8**, and methyl 2-cyanoacetate. ^{1}H NMR ($CDCl_3$) δ 10.99 (s, 0.5H), 10.06 (s, 1H), 7.98 (s, 0.5H), 7.58 (d, 1H, J = 7.7 Hz), 7.13−7.24 (m, 2H), 6.95−7.05 (m, 1H), 5.95 (br s, 0.5H), 5.14 (br s, 0.5H), 4.25 (br s, 1H), 3.96 (d, 1H, J = 16 Hz), 3.75 (s, 3H), 3.23−3.46 (m, 6H), 3.05−3.17 (m, 1H), 1.25−1.95 (m, 10H) ppm; ^{13}C NMR ($CDCl_3$) δ 172.91, 170.93, 165.71, 162.54, 130.32, 129.90, 127.53, 122.54, 120.78, 120.44, 119.01, 118.21, 106.68, 99.89, 55.12, 52.21, 51.54, 50.29, 46.06, 45.70, 36.48, 30.63, 26.29, 26.10, 24.00 ppm. HRMS for $C_{25}H_{29}ClN_6O_4$ calcd for $(M + H)^+$, 513.2017; measured, 513.2010. Anal. ($C_{25}H_{29}ClN_6O_4$) C, H, Cl, N.

(*S*)-2-Cyano-*N*,*N*′-dimethyl-3-(3-methyl-1*H*-indol-7-ylamino)-3-(2-oxo-1-(2-oxo-2-(pyrrolidin-1-yl)ethyl)azepan-3-ylamino)acrylamide (19). This compound was prepared in 81% yield from **7b**, **8**, and 2-cyano-*N*,*N*′-dimethylacetamide. ^{1}H NMR ($CDCl_3$) δ 11.58 (s, 0.5H), 9.41 (s, 0.5H), 7.99 (s, 1H), 7.46 (d, 1H, J = 8.2 Hz), 7.08 (t, 1H, J = 7.4 Hz), 6.99 (d, 1H, J = 7.7 Hz), 6.96 (s, 1H), 6.07 (br s, 0.5H), 4.94 (br s, 0.5H), 4.18 (br s, 1H), 4.02 (d, 1H, J = 15.3 Hz), 3.32−3.45 (m, 6H), 3.15 (br s, 1H), 3.06 (s, 6H), 2.29 (s, 3H), 1.39−1.98 (m, 10H) ppm; ^{13}C NMR ($CDCl_3$) δ 172.87, 165.81, 160.74, 152.16, 146.64, 139.99, 130.97, 130.38, 122.80, 119.32, 118.33, 117.83, 111.98, 99.41, 54.76, 51.72, 50.25, 46.04, 45.72, 38.34, 38.22, 30.29, 26.53, 26.26, 24.02, 9.72 ppm. HRMS for $C_{27}H_{35}N_7O_3$ calcd for $(M + H)^+$, 506.2880; measured, 506.2883. Anal. ($C_{27}H_{35}N_7O_3$) C, H, N.

(*S*)-3-(3-Chloro-1*H*-indol-7-ylamino)-2-cyano-*N*,*N*′-dimethyl-3-(2-oxo-1-(2-oxo-2-(pyrrolidin-1-yl)ethyl)azepan-3-ylamino)acrylamide (20). This compound was prepared in 90% yield from **7c**, **8**, and 2-cyano-*N*,*N*′-dimethylacetamide. ^{1}H NMR ($CDCl_3$) δ 11.55 (br s, 1H), 10.30 (br s, 0.6H), 7.52 (d, 1H, J = 7.7 Hz), 7.13−7.17 (m, 2H), 7.05 (d, 1H, J = 7.7 Hz), 5.68 (br s, 0.4H), 4.95 (br s, 1H), 4.20 (br s, 1H), 4.04 (d, 1H, J = 16.5 Hz), 3.71 (s, 1H), 3.34−3.45 (m, 4H), 3.13−3.20 (m, 1H), 3.05 (s, 7H), 1.97 (quintet, 2H, J = 6.6 Hz), 1.85 (quintet, 2H, J = 6.6 Hz), 1.45−1.80 (m, 6H) ppm; ^{13}C NMR ($CDCl_3$) δ 173.11, 167.13, 160.59, 152.51, 148.79, 137.18, 131.19, 127.35, 122.23, 120.66, 119.51, 117.16, 111.27, 106.42, 56.88, 52.01, 51.93, 50.39, 46.10, 45.72, 38.30, 31.77, 30.29, 26.67, 26.16, 24.04 ppm. HRMS for $C_{26}H_{32}ClN_7O_3$ calcd for $(M + H)^+$, 526.2333; measured, 526.2328. Anal. ($C_{26}H_{32}ClN_7O_3$) C, H, Cl, N.

(*S*)-3-(3-bromo-1*H*-indol-7-ylamino)-2-cyano-*N*,*N*′-dimethyl-3-(2-oxo-1-(2-oxo-2-(pyrrolidin-1-yl)ethyl)azepan-3-ylamino)acrylamide (21). This compound was prepared in 93% yield from **7e**, **8**, and 2-cyano-*N*,*N*′-dimethylacetamide. ^{1}H NMR ($CDCl_3$) δ 11.49 (br s, 0.5H), 10.40 (br s, 0.5H), 7.42 (d, 1H, J = 7.7 Hz), 7.16 (s, 1H), 7.11 (t, 1H, J = 7.4 Hz), 7.00 (d, 1H, J = 7.1 Hz), 5.70 (br s, 0.5H), 4.90 (br s, 0.5H), 4.14 (br s, 1H), 3.98 (d, 1H, J = 14.9 Hz), 3.52 (br s, 1H), 3.28−3.43 (m, 5H), 3.12 (d, 1H, J = 12.1 Hz), 3.00 (s, 6H), 1.37−1.95 (m, 10H) ppm; ^{13}C NMR ($CDCl_3$) δ 173.07, 171.23, 165.63, 160.60, 131.31, 129.94, 128.81, 125.33, 124.74, 121.61, 120.76, 119.46, 118.09, 91.04, 55.06, 51.97, 50.39, 50.25, 46.08, 45.70, 43.41, 38.32, 30.27, 26.67, 26.14, 24.02 ppm. HRMS for $C_{26}H_{32}BrN_7O_3$ calcd for $(M + H)^+$, 570.1828; measured, 570.1823. Anal. ($C_{26}H_{32}BrN_7O_3$) C, H, N.

(*S*)-3-(3-Cyano-1*H*-indol-7-ylamino)-2-cyano-*N*,*N*′-dimethyl-3-(2-oxo-1-(2-oxo-2-(pyrrolidin-1-yl)ethyl)azepan-3-ylamino)-acrylamide (22). This compound was prepared in 85% yield from **7f**, **8**, and 2-cyano-*N*,*N*′-dimethylacetamide. ^{1}H NMR ($CDCl_3$) δ 11.68 (br s, 0.6H), 11.51 (br s, 0.6H), 7.70 (s, 1H), 7.65 (d, 1H, J = 7.7 Hz), 7.14−7.24 (m, 2H), 7.11 (d, 1H, J = 7.7 Hz), 5.41 (br s, 0.4H), 5.01 (br s, 0.4H), 4.03−4.20 (m, 1H), 3.07−3.70 (m, 7H), 3.04 (s, 6H), 2.90−2.99 (m, 1H), 1.45−1.97 (m, 10H) ppm; ^{13}C NMR ($CDCl_3$) δ 173.37, 165.53, 157.74, 133.26, 129.19, 129.01, 128.20, 125.27, 124.22, 122.64, 121.32, 120.52, 118.41, 115.70, 87.39, 55.36, 52.23, 50.55, 46.20, 45.74, 38.24, 30.24, 26.79, 26.12, 24.02 ppm. HRMS for $C_{27}H_{32}N_8O_3$ calcd for $(M + H)^+$, 517.2676; measured, 517.2665. Anal. ($C_{27}H_{32}N_8O_3$) C, H, N.

(*S*)-7-(2-Cyano-3-(dimethylamino)-3-oxo-1-(2-oxo-1-(2-oxo-2-(pyrrolidin-1-yl)ethyl)azepan-3-ylamino)prop-1-enylamino)-1*H*-indole-3-carboxamide (23). This compound was prepared in 35% yield from **7g**, **8**, and 2-cyano-*N*,*N*′-dimethylacetamide. ^{1}H NMR ($CDCl_3$) δ 11.55 (br s, 1H), 10.30 (br s, 1H), 7.70 (s, 1H), 7.65 (d, 1H, J = 7.7 Hz), 7.14−7.24 (m, 2H), 7.11 (d, 1H, J = 7.7 Hz), 6.56 (br s, 1H), 5.41 (br s, 1H), 4.03−4.20 (m,

1H), 3.07−3.70 (m, 8H), 3.04 (s, 6H), 1.45−1.97 (m, 10H) ppm. HRMS for $C_{27}H_{34}N_8O_4$ calcd for $(M + H)^+$, 535.2781; measured, 535.2777. Anal. ($C_{27}H_{34}N_8O_4$) C, H, N.

(*S*)-1-(3-Methyl-1*H*-indol-7-yl)-2-cyano-3-(2-oxo-1-(2-oxo-2-(pyrrolidin-1-yl)ethyl)azepan-3-yl)guanidine (25). This compound was prepared in 83% yield from **7b**, **8**, and sodium cyanoamide. ^{1}H NMR ($CDCl_3$) δ 9.87 (s, 1H), 8.03 (s, 1H), 7.47 (d, 1H, J = 7.7 Hz), 7.06 (t, 1H, J = 7.7 Hz), 6.99 (d, 1H, J = 7.7 Hz), 6.98 (s, 1H), 6.36 (d, 1 H, J = 6.0 Hz), 4.58−4.62 (m, 1H), 4.11 (d, 1H, J = 16.5 Hz), 4.06 (d,1H, J = 16.5 Hz), 3.65 (dd, 1H, J = 14.5, 10.4 Hz), 3.24−3.38 (m, 5H), 3.22 (br d, 1H, J = 12.6 Hz), 2.30 (s, 3H), 1.99 (d, 1H, J = 12.6 Hz), 1.91 (quintet, 2H, J = 6.6 Hz), 1.55−1.81 (m, 6H), 1.41−1.48 (m, 1H) ppm; ^{13}C NMR ($CDCl_3$) δ 173.01, 166.03, 157.24, 131.33, 130.83, 123.14, 119.24, 118.96, 118.43, 118.21 (2C), 111.82, 54.49, 51.54, 50.45, 46.02, 45.70, 31.20, 27.54, 26.57, 26.10, 23.98, 9.66 ppm. HRMS for $C_{23}H_{29}N_7O_2$ calcd for $(M + H)^+$, 436.2461; measured, 436.2455. Anal. ($C_{23}H_{29}N_7O_2$) C, H, N.

(*S*)-1-(3-Chloro-1*H*-indol-7-yl)-2-cyano-3-(2-oxo-1-(2-oxo-2-(pyrrolidin-1-yl)ethyl)azepan-3-yl)guanidine (26). This compound was prepared in 87% yield from **7c**, **8**, and sodium cyanoamide. ^{1}H NMR ($CDCl_3$) δ 10.54 (s, 1H), 8.24 (s, 1H), 7.52 (d, 1H, J = 8.3 Hz), 7.17 (d, 1H, J = 2.2 Hz), 7.11 (t, 1H, J = 7.7 Hz), 7.05 (d, 1H, J = 7.7 Hz), 6.44 (d, 1 H, J = 6.1 Hz), 4.58−4.66 (m, 1H), 4.11 (d, 1H, J = 16.0 Hz), 4.03 (d,1H, J = 16.0 Hz), 3.66 (dd, 1H, J = 15.1, 11.3 Hz), 3.27−3.41 (m, 5H), 3.19 (dd, 1H, J = 15.1, 2.8 Hz), 2.04 (d, 1H, J = 11.6 Hz), 1.91 (quintet, 2H, J = 6.6 Hz), 1.40−1.81 (m, 7H) ppm; ^{13}C NMR ($CDCl_3$) δ 173.03, 165.89, 156.98, 130.00, 127.67, 122.44, 120.46, 119.83, 119.02, 118.09, 117.62, 106.62, 54.57, 51.62, 50.61, 46.02, 45.68, 31.26, 27.54, 26.57, 26.08, 23.96 ppm. HRMS for $C_{22}H_{26}ClN_7O_2$ calcd for $(M + H)^+$, 456.1915; measured, 456.1910. Anal. ($C_{22}H_{26}ClN_7O_2$) C, H, Cl., N.

Acknowledgment. We thank Drs. P. T. Cheng, P. Y. S. Lam, D. L. Cheney, and R. R. Wexler for insightful review of this work.

Supporting Information Available: Details of the enzymatic assays, EC_{2xPT} measurements, and plasma protein binding measurements, combustion analysis data for compounds **2**, **3**, **14**−**23**, **25**, and **26**, and crystallization details of FXa with **18**. This material is available free of charge via the Internet at http://pubs.acs.org.

References

(1) (a) Murray, C. J. L.; Lopez, A. D. Mortality by cause for eight regions of the world: Global Burden of Disease Study. *Lancet* **1997**, *349*, 1269–1276. (b) White, R. H. The epidemiology of venous thromboembolism. *Circulation* **2003**, *107*, I4–I8.

(2) Warfarin: (*RS*)-4-hydroxy-3-(3-oxo-1-phenylbutyl)coumarin.

(3) Herman, D.; Locatelli, I.; Grabnar, I.; Peternel, P.; Stegnar, M.; Mrhar, A.; Breskvar, K.; Dolzan, V. Influence of CYP2C9 polymorphisms, demographic factors and concomitant drug therapy on warfarin metabolism and maintenance dose. *Pharmacogenomics J.* **2005**, *5*, 193–202.

(4) (a) Lormeau, J. C.; Goulay, J.; Choay, J. Pharmaceutical Mucopolysaccharide Fraction. DE 2944792, 1980. (b) Glover, G. I.; Schasteen, C. S. Serine Protease Inhibitors. EP 238473, 1987.

(5) For reviews, see the following: (a) Zhu, B.-Y.; Scarborough, R. M. Recent advances in inhibitors of factor Xa in the prothrombinase complex. *Curr. Opin. Cardiovasc., Pulm., Renal Invest. Drugs* **1999**, *1*, 63–87. (b) Vacca, J. P. Thrombosis and coagulation. *Annu. Rep. Med. Chem.* **1998**, *33*, 81–90. (c) Kunitada, S.; Nagahara, T.; Hara, T. Inhibitors of factor Xa. *Handb. Exp. Pharmacol.* **1999**, *132*, 397–420. (d) Ewing, W. R.; Pauls, H. W.; Spada, A. P. Progress in the design of inhibitors of coagulation factor Xa. *Drugs Future* **1999**, *24*, 771–787. (e) Fevig, J. M.; Wexler, R. R. Anticoagulants: Thrombin and factor Xa inhibitors. *Annu. Rep. Med. Chem.* **1999**, *34*, 81–100. (f) Betz, A. Recent advances in factor Xa inhibitors. *Expert Opin. Ther. Pat.* **2001**, *11*, 1007–1017. (g) Casimiro-Garcia, A.; Dudley, D. A.; Heemstra, R. J.; Filipski, K. J.; Bigge, C. F.; Edmunds, J. J. Progress in the discovery of factor Xa inhibitors. *Expert Opin. Ther. Pat.* **2006**, *16*, 119–145.

(6) (a) Walsh, P. N. Roles of factor XI, platelets and tissue factor-initiated blood coagulation. *J. Thromb. Haemostasis* **2003**, *1*, 2081–2086. (b) Hoffman, M.; Monroe, D. M., III. A cell-based model of hemostasis. *Thromb. Haemostasis* **2001**, *85*, 958–965.

(7) (a) Quan, M. L.; Lam, P. Y. S.; Han, Q.; Pinto, D. J. P.; He, M. Y.; Li, R.; Ellis, C. D.; Clark, C. G.; Teleha, C. A.; Sun, J.-H.; Alexander, R. S.; Bai, S.; Luettgen, J. M.; Knabb, R. M.; Wong, P. C.; Wexler, R. R. Discovery of 1-(3′-aminobenzisoxazol-5′-yl)-3-trifluoromethyl-*N*-[2-fluoro-4-[(2′-dimethylaminomethyl)imidazol-1-yl]phenyl]-1*H*-pyrazole-5-carboxyamide hydrochloride (razaxaban), a highly potent, selective, and orally bioavailable factor Xa inhibitor. *J. Med. Chem.* **2005**, *48*, 1729–1744. (b) Pinto, D. J. P.; Orwat, M. J.; Wang, S.; Fevig, J. M.; Quan, M. L.; Amparo, E.; Cacciola, J.; Rossi, K. A.; Alexander, R. S.; Smallwood, A. M.; Luettgen, J. M.; Liang, L.; Aungst, B. J.; Wright, M. R.; Knabb, R. M.; Wong, P. C.; Wexler, R. R.; Lam, P. Y. S. Discovery of 1-[3-(aminomethyl)phenyl]-*N*-[3-fluoro-2′-(methylsulfonyl)-[1,1′-biphenyl]-4-yl]-3-(trifluoromethyl)-1*H*-pyrazole-5-carboxamide (DPC423), a highly potent, selective, and orally bioavailable inhibitor of blood coagulation factor Xa. *J. Med. Chem.* **2001**, *44*, 566–578. (c) Lam, P. Y. S.; Clark, C. G.; Li, R.; Pinto, D. J. P.; Orwat, M. J.; Galemmo, R. A.; Fevig, J. M.; Teleha, C. A.; Alexander, R. S.; Smallwood, A. M.; Rossi, K. A.; Wright, M. R.; Bai, S. A.; He, K.; Luettgen, J. M.; Wong, P. C.; Knabb, R. M.; Wexler, R. R. Structure-based design of novel guanidine/benzamidine mimics: potent and orally bioavailable factor Xa inhibitors as novel anticoagulants. *J. Med. Chem.* **2003**, *46*, 4405–4418. (d) Lassen, M. R.; Davidson, B. L.; Gallus, A.; Pineo, G.; Ansell, J.; Deitchman, D. A phase II randomized, double-blind, five-arm, parallel-group, dose-response study of a new oral directly-acting factor Xa inhibitor, razaxaban, for the prevention of deep vein thrombosis in knee replacement surgery—on behalf of the razaxaban investigators. *Blood* **2003**, *102*, Abs 41. (e) Wong, P. C.; Crain, E. J.; Watson, C. A.; Wexler, R. R.; Lam, P. Y. S.; Quan, M. L.; Knabb, R. M. Razaxaban, a direct factor Xa inhibitor, in combination with aspirin and/or clopidogrel improves low-dose antithrombotic activity without enhancing bleeding liability in rabbits. *J. Thromb. Thrombolysis* **2007**, *24*, 43–51.

(8) (a) Pinto, D. J. P.; Orwat, M. J.; Koch, S.; Rossi, K. A.; Alexander, R. S.; Smallwood, A.; Wong, P. C.; Rendina, A. R.; Luettgen, J. M.; Knabb, R. M.; He, K.; Xin, B.; Wexler, R. R.; Lam, P. Y. S. Discovery of 1-(4-methoxyphenyl)-7-oxo-6-(4-(2-oxopiperidin-1-yl)phenyl)-4,5,6,7-tetrahydro-1*H*-pyrazolo[3,4-*c*]pyridine-3-carboxamide (Apixaban, BMS-562247), a highly potent, selective, efficacious, and orally bioavailable inhibitor of blood coagulation factor Xa. *J. Med. Chem.* **2007**, *50*, 5339–5356. (b) Wong, P. C.; Crain, E. J.; Xin, B.; Wexler, R. R.; Lam, P. Y.; Pinto, D. J.; Luettgen, J. M.; Knabb, R. M. Apixaban, an oral, direct and highly selective factor Xa inhibitor in vitro, antithrombotic and antihemostatic studies. *J. Thromb. Haemostasis* **2008**, *6*, 820–829.

(9) (a) Roehrig, S.; Straub, A.; Pohlmann, J.; Lampe, T.; Pernerstorfer, J.; Schlemmer, K.-H.; Reinemer, P.; Perzborn, E. Discovery of the novel antithrombotic agent 5-chloro-*N*-({(5*S*)-2-oxo-3- [4-(3-oxomorpholin-4-yl)phenyl]-1,3-oxazolidin-5-yl}methyl)thiophene-2-carboxamide (BAY 59-7939): an oral, direct factor Xa inhibitor. *J. Med. Chem.* **2005**, *48*, 5900–5908. (b) Eriksson, B. I.; Borris, L.; Dahl, O. E.; Haas, S.; Huisman, M. V.; Kakkar, A. K.; Misselwitz, F.; Kaelebo, P. Oral, direct factor Xa inhibition with BAY 59-7939 for the prevention of venous thromboembolism after total hip replacement. *J. Thromb. Haemostasis* **2006**, *4*, 121–128. (c) Kubitza, D.; Becka, M.; Wensing, G.; Voith, B.; Zuehlsdorf, M. Safety, pharmacodynamics, and pharmacokinetics of BAY 59-7939—an oral, direct factor Xa inhibitor—after multiple dosing in healthy male subjects. *Eur. J. Clin. Pharmacol.* **2005**, *61*, 873–880. (d) Turpie, A. G. G.; Fisher, W. D.; Bauer, K. A.; Kwong, L. M.; Irwin, M. W.; Kalebo, P.; Misselwitz, F.; Gent, M. BAY 59-7939: an oral, direct factor Xa inhibitor for the prevention of venous thromboembolism in patients after total knee replacement. A phase II dose-ranging study. *J. Thromb. Haemostasis* **2005**, *3*, 2479–2486.

(10) (a) Agnelli, G.; Haas, S. K.; Krueger, K. A.; Bedding, A. W.; Brandt, J. T. A phase II study of the safety and efficacy of a novel oral FXa inhibitor (LY517717) for the prevention of venous thromboembolism following TKR or THR. *ASH Annu. Meet. Abstr.* **2005**, *106*, 278. (b) Hampton, T. New oral anticoagulants show promise. *JAMA, J. Am. Med. Assoc.* **2006**, *295*, 743–744. (c) Liebeschuetz, J. W.; Jones, S. D.; Wiley, M. E.; Young, S. C. Iterative structure-based screen of virtual chemical libraries and factor Xa: finding the oral available antithrombotic candidate LY517717. *Struct.-Based Drug Discovery* **2006**, 173–192.

(11) (a) Shi, Y.; Zhang, J.; Stein, P. D.; Shi, M.; O'Connor, S. P.; Bisaha, S. N.; Li, C.; Atwal, K. S.; Bisacchi, G. S.; Sitkoff, D.; Pudzianowski, A. T.; Liu, E. C.; Hartl, K. S.; Seiler, S. M.; Youssef, S.; Steinbacher, T. E.; Schumacher, W. A.; Rendina, A. R.; Bozarth, J. M.; Peterson, T. L.; Zhang, G.; Zahler, R. Ketene aminal-based lactam derivatives as a novel class of orally active FXa inhibitors. *Bioorg. Med. Chem. Lett.* **2005**, *15*, 5453–5458. (b) Bisacchi, G. S.; Stein, P. D.; Gougoutas,

J. Z.; Hartl, K. S.; Lawrence, R. M.; Liu, E. C.; Pudzianowski, A. T.; Schumacher, W. A.; Sitkoff, D.; Steinbacher, T. E.; Sutton, J.; Zhang, Z.; Seiler, S. M. Initial structure−activity relationships for a caprolactam-based series of neutral factor Xa inhibitors: lead identification. *Lett. Drug Des. Discovery* **2005**, *2*, 625–630. (c) Stein, P. D.; Shi, Y.; O'Connor, S. P.; Li, C. Preparation of Lactam Inhibitors of Factor Xa. WO 2001096331, 2001.

(12) Masters, J. J.; Franciskovich, J. B.; Tinsley, J. M.; Campbell, C.; Campbell, J. B.; Craft, T. J.; Froelich, L. L.; Gifford-Moore, D. S.; Hay, L. A.; Herron, D. K.; Klimkowski, V. J.; Kurz, K. D.; Metz, J. T.; Ratz, A. M.; Shuman, R. T.; Smith, G. F.; Smith, T.; Towner, R. D.; Wiley, M. R.; Wilson, A.; Yee, Y. K. Non-amidine-containing 1,2-dibenzamidobenzene inhibitors of human factor Xa with potent anticoagulant and antithrombotic activity. *J. Med. Chem.* **2000**, *43*, 2087–2092.

(13) Compound **2** is inactive ($IC_{50} > 33\ \mu M$) when tested against thrombin, trypsin, factor IXa, factor VIIa, plasmin, and urokinase; intravenous bolus injection of 10 mg/kg of **2** led to a 1.8-, 1.4-, and 1.1-fold increase in prothrombin time (PT) after 5, 20 and 60 min, respectively.

(14) (a) IARC. *Monographs on the Evaluation of the Carcinogenic Risk of Chemicals to Man*; IARC Press: Lyon, France, 1995; p 431. (b) Burka, L. T.; Boyd, M. R. Furans. *Bioact. Foreign Compd.* **1985**, 243–257.

(15) Kratochwil, N. A.; Huber, W.; Mueller, F.; Kansy, M.; Gerber, P. R. Predicting plasma protein binding of drugs—revisited. *Curr. Opin. Drug Discovery Dev.* **2004**, *7*, 507–512.

(16) (a) Tucker, T. J.; Lumma, W. C.; Lewis, S. D.; Gardell, S. J.; Lucas, B. J.; Baskin, E. P.; Woltmann, R.; Lynch, J. J.; Lyle, E. A.; Appleby, S. D.; Chen, I. W.; Dancheck, K. B.; Vacca, J. P. Potent noncovalent thrombin inhibitors that utilize the unique amino acid D-dicyclohexylalanine in the P3 position. Implications on oral bioavailability and antithrombotic efficacy. *J. Med. Chem.* **1997**, *40*, 1565–1569. (b) Zhang, P.; Bao, L.; Zuckett, J. F.; Goldman, E. A.; Jia, Z. J.; Arfsten, A.; Edwards, S.; Sinha, U.; Hutchaleelaha, A.; Park, G.; Lambing, J. L.; Hollenbach, S. J.; Scarborough, R. M.; Zhu, B.-Y. Design, synthesis, and SAR of anthranilamide-based factor Xa inhibitors incorporating substituted biphenyl P4 motifs. *Bioorg. Med. Chem. Lett.* **2004**, *14*, 983–987. (c) Chou, Y.-L.; Davey, D. D.; Eagen, K. A.; Griedel, B. D.; Karanjawala, R.; Phillips, G. B.; Sacchi, K. L.; Shaw, K. J.; Wu, S. C.; Lentz, D.; Liang, A. M.; Trinh, L.; Morrissey, M. M.; Kochanny, M. J. Structure−activity relationships of substituted benzothiophene-anthranilamide factor Xa inhibitors. *Bioorg. Med. Chem. Lett.* **2003**, *13*, 507–511. (d) Hirayama, F.; Koshio, H.; Katayama, N.; Kurihara, H.; Taniuchi, Y.; Sato, K.; Hisamichi, N.; Sakai-Moritani, Y.; Kawasaki, T.; Matsumoto, Y.; Yanagisawa, I. The discovery of YM-60828: a potent, selective and orally-bioavailable factor Xa inhibitor. *Bioorg. Med. Chem.* **2002**, *10*, 1509–1523. (e) Sinha, U.; Lin, P. H.; Edwards, S. T.; Wong, P. W.; Zhu, B.; Scarborough, R. M.; Su, T.; Jia, Z. J.; Song, Y.; Zhang, P.; Clizbe, L.; Park, G.; Reed, A.; Hollenbach, S. J.; Malinowski, J.; Arfsten, A. E. Inhibition of purified factor Xa amidolytic activity may not be predictive of inhibition of in vivo thrombosis. *Arterioscler., Thromb., Vasc. Biol.* **2003**, *23*, 1098–1104. (f) Shi, Y.; Sitkoff, D.; Zhang, J.; Han, W.; Hu, Z.; Stein, P. D.; Wang, Y.; Kennedy, L. J.; O'Connor, S. P.; Ahmad, S.; Liu, E. C.-K.; Seiler, S. M.; Lam, P. Y.S.; Robl, J. A.; Macor, J. E.; Atwal, K. S.; Zahler, R. Amino(methyl) pyrrolidines as novel scaffolds for factor Xa inhibitors. *Bioorg. Med. Chem. Lett.* **2007**, *17*, 5952–5958.

(17) For early examples, see the following: (a) Tucker, T. J.; Brady, S. F.; Lumma, W. C.; Lewis, S. D.; Gardell, S. J.; Naylor-Olsen, A. M.; Yan, Y.; Sisko, J. T.; Stauffer, K. J.; Lucas, B. J.; Lynch, J. J.; Cook, J. J.; Stranieri, M. T.; Holahan, M. A.; Lyle, E. A.; Baskin, E. P.; Chen, I.-W.; Dancheck, K. B.; Krueger, J. A.; Cooper, C. M.; Vacca, J. P. Design and synthesis of a series of potent and orally bioavailable noncovalent thrombin inhibitors that utilize nonbasic groups in the P1 position. *J. Med. Chem.* **1998**, *41*, 3210–3219. (b) Maignan, S.; Guilloteau, J.-P.; Choi-Sledeski, Y. M.; Becker, M. R.; Ewing, W. R.; Pauls, H. W.; Spada, A. P.; Mikol, V. Molecular structures of human factor Xa complexed with ketopiperazine inhibitors: preference for a neutral group in the S1 pocket. *J. Med. Chem.* **2003**, *46*, 685–690. (c) Adler, M.; Kochanny, M. J.; Ye, B.; Rumennik, G.; Light, D. R.; Biancalana, S.; Whitlow, M. Crystal structures of two potent nonamidine inhibitors bound to factor Xa. *Biochemistry* **2002**, *41*, 15514–15523.

(18) (a) Sitkoff, D. Probing the source of the exceptional role played by chlorine in the FXa S1 pocket. *Abstr. Pap.—Am. Chem. Soc.* **2006**, *232*, COMP-075. (232nd National Meeting of the American Chemical Society, Division of Computational Chemistry, San Fancisco, CA, September, 2006). (b) Chan, C.; Borthwick, A. D.; Brown, D.; Burns-Kurtis, C. L.; Campbell, M.; Chaudry, L.; Chung, C.-w.; Convery, M. A.; Hamblin, N.; Johnstone, L.; Kelly, H. A.; Kleanthous, S.; Patikis, A.; Patel, C.; Pateman, A. J.; Senger, S.; Shah, G. P.; Toomey, J. R.; Watson, N. S.; Weston, H. E.; Whitworth, C.; Youg, R. J.; Zhou, P. Factor Xa inhibitors: S1 binding interactions of a series of *N*-{(3*S*)-1-[(1*S*)-1-methyl-2-morpholin-4-yl-2-oxoethyl]-2-oxopyrrolidin-3-yl}sulfonamides. *J. Med. Chem.* **2007**, *50*, 1546–1557.

(19) Gly218 is sometimes referred to as Gly219 in the literature depending on how the FXa sequence was aligned with that of chymotripsinogen, on which the numbering system is based.

(20) Subsequent to our discovery of the 7-linked 3-chloroindole P1 pharmacophore,[11c] several reports and crystal structures of a 2-linked-5-chloroindole P1 group that fills the base of the S1 pocket and hydrogen bonds to Gly218 carbonyl have appeared: Komoriya, S.; Haginoya, N.; Kobayashi, S.; Nagata, T.; Mochizuki, A.; Suzuki, M.; Yoshino, T.; Horino, H.; Nagahara, T.; Suzuki, M.; Isobe, Y.; Furugoori, T. Design, synthesis, and biological activity of non-basic compounds as factor Xa inhibitors: SAR study of S1 and aryl binding sites. *Bioorg. Med* **2005**, *13*, 3927–3954. Nagata, T.; Yoshino, T.; Haginoya, N.; Yoshikawa, K.; Isobe, Y.; Furugohri, T.; Kanno, H. Cycloalkanediamine derivatives as novel blood coagulation factor Xa inhibitors. *Bioorg. Med. Chem. Lett.* **2007**, *17*, 4683–4688. Additionally, there are several examples of amide-linked para-chlorophenyl P1 groups in which the NH of the amide linker forms a hydrogen bond to Gly218 carbonyl (earliest examples are pdb entries 1mk5 and 1mk6 from 2003). Recently, Qiao et al. reported a ligand with a 6-linked 3-chloroindole P1 group crystallized in FXa. As expected, the primary hydrogen bond is to Asp189; there is, however, a secondary, weak (3.5 Å) interaction to Gly218 carbonyl. See the following: Qiao, J. X.; Chang, C.-H.; Cheney, D. L.; Morin, P. E.; Wang, G. Z.; King, S. R.; Wang, T. C.; Rendina, A. R.; Luettgen, J. M.; Knabb, R. M.; Wexler, R. R.; Lam, P. Y. S. SAR and X-ray structures of enantiopure 1,2-*cis*-(1*R*,2*S*)-cyclopentyldiamine and cyclohexyldiamine derivatives as inhibitors of coagulation factor Xa. *Bioorg. Med. Chem. Lett.* **2007**, *17*, 4419–4427.

(21) The clogP values are calculated with Biobyte clogP, version 4.2, using version 22 of the associated fragment database. For both compounds **2** and **3**, the software used an approximated fragment value (error code 30). For comparison, the clogP values for 3-methylindole and 2-methylbenzofuran are 2.6 and 3.2 with no errors codes reported, following the same trend as the values for the complete compounds **3** and **2**. This suggests that the approximated fragment is likely in the non-S1, or constant portion of the compounds, and that difference in clogP for the complete compounds is measuring the 3-methylindole versus 2-methylbenzofuran contribution.

(22) Owa, T.; Yoshino, H.; Okauchi, T.; Yoshimatsu, K.; Ozawa, Y.; Sugi, N. H.; Nagasu, T.; Koyanagi, N.; Kitoh, K. Discovery of novel antitumor sulfonamides targeting G1 phase of the cell cycle. *J. Med. Chem.* **1999**, *42*, 3789–3799.

(23) Shi, Y.; Zhang, J.; Grazier, N.; Stein, P. D.; Atwal, K. S.; Traeger, S. C.; Callahan, S. P.; Malley, M. F.; Galella, M. A.; Gougoutas, J. Z. One-pot synthesis and conformational features of *N,N′*-disubstituted ketene aminals. *J. Org. Chem.* **2004**, *69*, 188–191.

(24) Atwal, K. S.; Ahmed, S. Z.; O'Reilly, B. C. A facile synthesis of cyanoguanidines from thioureas. *Tetrahedron Lett.* **1989**, *30*, 7313–7316.

(25) Among all currently available pdb structures of FXa, only structure 1iqe has its Ser195 side chain modeled in a position similar to that observed in the crystal structure of **18**. 1iqe is a 2.9 Å resolution structure; unfortunately, there is no associated publication to document and discuss the finding, and the structure factors were not submitted to the pdb.

(26) An additional notable finding is that in one of the two structures in the asymmetric unit of the crystal structure of **18**, the conserved water that is usually found in S4 is missing; there is no obvious reason for its absence.

(27) Herron, D. K.; Goodson, T. J.; Wiley, M. R.; Weir, L. C.; Kyle, J. A.; Yee, Y. K.; Tebbe, A. L.; Tinsley, J. M.; Mendel, D.; Masters, J. J.; Franciskovich, J. B.; Sawyer, J. S.; Beight, D. W.; Ratz, A. M.; Milot, G.; Hall, S. E.; Klimkowski, V. J.; Wikel, J. H.; Eastwood, B. J.; Towner, R. D.; Gifford-Moore, D. S.; Craft, T. J.; Smith, G. F. 1,2-Dibenzamidobenzene inhibitors of human factor Xa. *J. Med. Chem.* **2000**, *43*, 859–872.

(28) (a) Matter, H.; Will, D. W.; Nazare, M.; Schreuder, H.; Laux, V.; Wehner, V. Structural requirements for factor Xa inhibition by 3-oxybenzamides with neutral P1 substituents: combining X-ray crystallography, 3D-QSAR, and tailored scoring functions. *J. Med. Chem.* **2005**, *48*, 3290–3312. (b) Frédérick, R.; Robert, S; Charlier, C.; Wouters, J.; Masereel, B.; Pochet, L. Mechanism-based thrombin inhibitors: design, synthesis, and molecular docking of a new selective 2-oxo-2*H*-1-benzopyran derivative. *J. Med. Chem.* **2007**, *50*, 3645–3650.

(29) (a) Imai, Y. N.; Inoue, Y.; Nakanishi, I.; Kitaura, K. Cl−π interactions in protein−ligand complexes. *Protein Sci.* **2008**, *17*, 1129–1137. (b) Tsuzuki, S.; Honda, K.; Uchimaru, T.; Mikami, M.; Tanabe, K. The magnitude of the CH/π interaction between benzene and some model hydrocarbons. *J. Am. Chem. Soc.* **2000**, *122*, 3746–3753. (c) Ringer,

A. L.; Figgs, M. S.; Sinnokrot, M. O.; Sherrill, C. D. Aliphatic C-H/π interactions: methane−benzene, methane−phenol, and methane−indole complexes. *J. Phys. Chem. A* **2006**, *110*, 10822–10828.

(30) Swiss Webster mice (24−38 g) were anesthetized with sodium pentobarbital (100 mg/kg, ip). Russell's viper venom (Sigma Chemical Co., St. Louis, MO) was prepared in 0.9% saline and injected into the tail vein at a dose of 7 μg/mouse in a volume of 0.1 mL given 15 min after induction of anesthesia. This dose of venom was found to be uniformly fatal in 105 mice with death occurring in an average of 1.5 ± 1.9 min (±SD, range was 1−12 min with 88% of mice dying within 2 min). Histological evaluation of several venom-treated mice revealed that early death was due to occlusion of pulmonary capillaries with fibrin aggregates, probably caused by initiation of blood coagulation by venom activation of factor X to factor Xa. A 5 mg/kg dose of test compounds or saline vehicle was administered by oral gavage 45 min before the venom injection. Survival was monitored out to 30 min after venom injection.

(31) Quan, M. L.; Smallheer, J. M. The race to an orally active factor Xa inhibitor: recent advances. *Curr. Opin. Drug Discovery Dev.* **2004**, *7*, 460–469.

(32) Adler, M.; Davey, D. D.; Phillips, G. B.; Kim, S.-H.; Jancarik, J.; Rumennik, G.; Light, D. R.; Whitlow, M. Preparation, characterization, and the crystal structure of the inhibitor ZK-807834 (CI-1031) complexed with factor Xa. *Biochemistry* **2000**, *39*, 12534–12542.

(33) (a) Dinur, U.; Hagler, A. T. New Approaches to Empirical Forcefields. In *Reviews in Computational Chemistry*; Lipkowitz, K. B., Boyd, D. B., Eds; VCH Publishers: New York, 1991; Vol. 2, pp 99−164. (b) Maple, J. R.; Hwang, M. J.; Stockfisch, T. P.; Dinur, U.; Waldman, M.; Ewig, C. S.; Hagler, A. T. Derivation of class II forcefields. I. Methodology and quantum forcefield for the alkyl function group and alkane molecules. *J. Comput. Chem.* **1994**, *15*, 162–182.

(34) *Jaguar*, version 6.5; Schrodinger, LLC: New York, 2005.

(35) Frisch, M. J.; Trucks, G. W.; Schlegel, H. B.; Scuseria, G. E.; Robb, M. A.; Cheeseman, J. R.; Montgomery, J. A., Jr.; Vreven, T.; Kudin, K. N.; Burant, J. C.; Millam, J. M.; Iyengar, S. S.; Tomasi, J.; Barone, V.; Mennucci, B.; Cossi, M.; Scalmani, G.; Rega, N.; Petersson, G. A.; Nakatsuji, H.; Hada, M.; Ehara, M.; Toyota, K.; Fukuda, R.; Hasegawa, J.; Ishida, M.; Nakajima, T.; Honda, Y.; Kitao, O.; Nakai, H.; Klene, M.; Li, X.; Knox, J. E.; Hratchian, H. P.; Cross, J. B.; Bakken, V.; Adamo, C.; Jaramillo, J.; Gomperts, R.; Stratmann, R. E.; Yazyev, O.; Austin, A. J.; Cammi, R.; Pomelli, C.; Ochterski, J. W.; Ayala, P. Y.; Morokuma, K.; Voth, G. A.; Salvador, P.; Dannenberg, J. J.; Zakrzewski, V. G.; Dapprich, S.; Daniels, A. D.; Strain, M. C.; Farkas, O.; Malick, D. K.; Rabuck, A. D.; Raghavachari, K.; Foresman, J. B.; Ortiz, J. V.; Cui, Q.; Baboul, A. G.; Clifford, S.; Cioslowski, J.; Stefanov, B. B.; Liu, G.; Liashenko, A.; Piskorz, P.; Komaromi, I.; Martin, R. L.; Fox, D. J.; Keith, T.; Al-Laham, M. A.; Peng, C. Y.; Nanayakkara, A.; Challacombe, M.; Gill, P. M. W.; Johnson, B.; Chen, W.; Wong, M. W.; Gonzalez, C.; Pople, J. A. *Gaussian 03*, revision D.01; Gaussian, Inc.: Wallingford, CT, 2004.

(36) Otwinowski, Z.; Minor, W. Processing of X-ray Diffraction Data Collected in Oscillation Mode. In *Methods in Enzymology, Macromolecular Crystallography, Part A*; Carter, C. W., Sweet, R. M., Eds.; Academic Press, Inc.: New York, 1997; Vol. 276, pp 307−326.

(37) French, S.; Wilson, K. On the treatment of negative intensity observations. *Acta Crystallogr.* **1978**, *A34*, 517–525.

(38) Bailey, S. The CCP4 suite: programs for protein crystallography. *Acta Crystallogr.* **1994**, *D50*, 760–763.

(39) Brünger, A. T.; Adams, P. D.; Clore, G. M.; DeLano, W. L.; Gros, P.; Grosse-Kunstleve, R. W.; Jiang, J.-S.; Kuszewski, J; Nilges, M; Pannu, N. S.; Read, R. J.; Rice, L. M.; Simonson, T.; Warren, G. L. Crystallography & NMR system: a new software suite for macromolecular structure determination. *Acta Crystallogr.* **1998**, *D54*, 905–921.

(40) Adams, P. D.; Grosse-Kunstleve, R. W.; Hung, L.-W.; Ioerger, T. R.; McCoy, A. J.; Moriarty, N. W.; Read, R. J.; Sacchettini, J. C.; Sauter, N. K.; Terwilliger, T. C. PHENIX: building new software for automated crystallographic structure determination. *Acta Crystallogr.* **2002**, *D58*, 1948–1954.

(41) Emsley, P.; Cowtan, K. COOT: model-building tools for molecular graphics. *Acta Crystallogr.* **2004**, *D60*, 2126–2132.

(42) Lovell, S. C.; Davis, I. W.; Arendall, W. B., III; de Bakker, P. I. W.; Word, J. M.; Prisant, M. G.; Richardson, J. S.; Richardson, D. C. Structure validation by Cα geometry: φ, ψ, and Cβ deviation. *Proteins: Struct., Funct., Genet.* **2003**, *50*, 437–450.

(43) Shao, Y.; Fusti-Molnar, L.; Jung, Y.; Kussmann, J.; Ochsenfeld, C.; Brown, S. T.; Gilbert, A. T. B.; Slipchenko, L. V.; Levchenko, S. V.; O'Neill, D. P.; Distasio, R. A., Jr.; Lochan, R. C.; Wang, T.; Beran, G. J. O.; Besley, N. A.; Herbert, J. M.; Lin, C. Y.; Van Voorhis, T.; Chien, S. H.; Sodt, A; Steele, R. P.; Rassolov, V. A.; Maslen, P. E.; Korambath, P. P.; Adamson, R. D.; Austin, B.; Baker, J.; Byrd, E. F. C.; Dachsel, H.; Doerksen, R. J.; Dreuw, A.; Dunietz, B. D.; Dutoi, A. D.; Furlani, T. R.; Gwaltney, S. R.; Heyden, A.; Hirata, S.; Hsu, C.-P.; Kedziora, G.; Khalliulin, R. Z.; Klunzinger, P.; Lee, A. M.; Lee, M. S.; Liang, W.; Lotan, I.; Nair, N.; Peters, B.; Proynov, E. I.; Pieniazek, P. A.; Rhee, Y. M.; Ritchie, J.; Rosta, E.; Sherrill, C. D.; Simmonett, A. C.; Subotnik, J. E.; Woodcock, H. L., III; Zhang, W.; Bell, A. T.; Chakraborty, A. K.; Chipman, D. M.; Keil, F. J.; Warshel, A.; Hehre, W. J.; Schaefer, H. F., III; Kong, J.; Krylov, A. I.; Gill, P. M. W.; Head-Gordon, M. Advances in methods and algorithms in a modern quantum chemistry program package. *Phys. Chem. Chem. Phys.* **2006**, *8*, 3172–3191.

(44) Berman, H. M.; Westbrook, J.; Feng, Z.; Gilliland, G.; Bhat, T. N.; Weissig, H.; Shindyalov, I. N.; Bourne, P. E. Protein data bank. *Nucleic Acids Res.* **2000**, *28*, 235–242.

JM800855X